



## Observation of orbital modulation of the VHE emission from the binary system LS 5039 with H.E.S.S.

MATHIEU DE NAUROIS<sup>1</sup>, GAVIN ROWELL<sup>2</sup> FOR THE H.E.S.S. COLLABORATION

<sup>1</sup>LPNHE IN2P3 - CNRS - Universits Paris VI et Paris VII, France

<sup>2</sup>School of Chemistry & Physics, University of Adelaide, Adelaide 5005, Australia

denauroi@in2p3.fr

**Abstract:** The binary system LS 5039 was serendipitously with the High Energy Stereoscopic system (H.E.S.S.) during the scan of the inner galactic plane in 2004. Deeper observations were carried out in 2005, and brought clear evidence for TeV emission periodicity. This is the highest energy periodic source known so far. The observed flux modulation is attributed to a modulated absorption of the VHE gamma-ray emission of the compact object through pair creation on the stellar photosphere. Spectral modulation is also observed in this system; this might have several origins such as modulation of particle acceleration or reprocessing of high energy photons towards lower energy through cascading.

We will present detailed studies of the source variability (flux and spectral shape), the timescales compared to other wavelengths, and briefly review the implications for existing emission models.

### Introduction

In the commonly accepted paradigm, microquasars consist of a compact object (black hole or neutron star) fed by a massive star. They can exhibit superluminal radio jets[1], and emission from the accretion disk. LS 5039, identified in 1997[2] as a massive X-ray binary system with faint radio emission[3], was resolved by Paredes et al.[4] into a bipolar radio outflow emanating from a central core, thus possibly placing it into the *microquasar class*. The detection of radio and variable X-ray emission[5] and its possible association with the EGRET source 3EG J1824-1514 suggested the presence of multi-GeV particles accelerated in jets. This binary system (Fig 1) consists of a massive O6.5V star in a  $\sim 3.9$  day mildly eccentric orbit ( $e = 0.35$ )[6] around a compact object whose exact nature (black hole or neutron star) is still under debate.

### H.E.S.S. Observations

The High Energy Stereoscopic System (H.E.S.S.) is an array of four Atmospheric Cherenkov Tele-

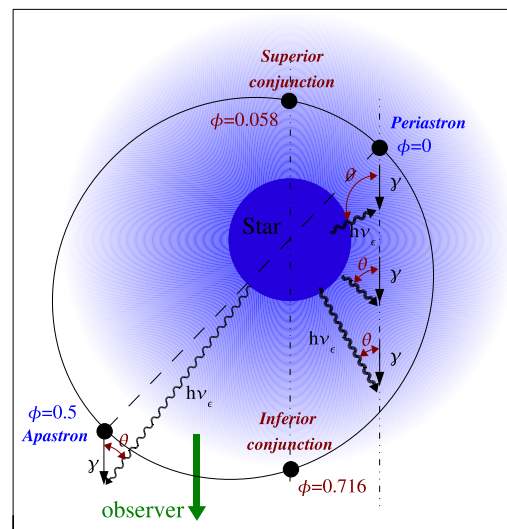


Figure 1: Orbital geometry of the binary system LS 5039 viewed from above and using the orbital parameters derived by Casares et al.[6]. Shown are: phases ( $\phi$ ) of minimum (*periastron*) and maximum (*apastron*) binary separation; epoch of superior and inferior conjunctions occurring when the compact object and the star are aligned along the observer's light-of-sight.

scopes (ACT)[7] located in the Southern Hemisphere (Namibia, 1800 m a.s.l.) and sensitive to  $\gamma$  rays above 100 GeV. LS 5039 was serendipitously detected in 2004 during the H.E.S.S. galactic scan[8]. The 2004 observations have been followed up by a deeper observation campaign[9] in 2005, leading to a total dataset of 69.2 hours of observation after data quality selection.

After selection cuts, a total of 1969  $\gamma$ -ray events were found within  $0.1^\circ$  of the VLBA radio position of LS 5039 (statistical significance of  $40\sigma$ ). The best fit position,  $l = 16.879^\circ$ ,  $b = -1.285^\circ$  is compatible with the VLBA position within uncertainties  $\pm 12''$  (stat.) and  $\pm 20''$  (syst.). We obtain an upper limit of  $28''$  (at  $1\sigma$ ) on the source size.

### Timing Analysis

The runwise VHE  $\gamma$ -ray flux at energies  $\geq 1$  TeV was decomposed into its frequency components using the Lomb-Scargle periodogram[10] (Fig. 2). A very significant peak (chance probability of  $\sim 10^{-20}$  before trials) occurs in the Lomb-Scargle periodogram at the period  $3.9078 \pm 0.0015$  days, consistent with the most recent optical orbital period[6] ( $3.90603 \pm 0.00017$  days). After sub-

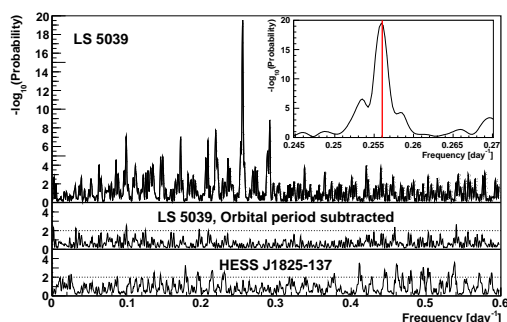


Figure 2: Lomb-Scargle (LS) periodogram of the VHE runwise flux of LS 5039 above 1 TeV (Chance probability to obtain the LS power vs. frequency). From [9]. Zoom: inset around the highest peak, which corresponds to a period of  $3.9078 \pm 0.0015$  days, compatible with the optical orbital period[6] denoted as a red line. Middle: LS periodogram of the same data after subtraction of a pure sinusoidal component (see text). Bottom: LS periodogram obtained on HESS J1825-137 observed in the same field of view.

traction of a pure sinusoid at the orbital period, the orbital peak disappears as expected (Fig. 2, middle), but also the numerous satellite peaks which correspond to beat periods of the orbital period with observation gaps (day-night cycle, moon period, annual period). The bottom panel of the same figure shows the result obtained on the neighbouring source HESS J1825-137 observed in the same field of view as LS 5039. The absence of any significant peak demonstrates that the observed periodicity is genuinely associated with LS 5039.

### Flux Modulation

The runwise Phasogram (Fig 3) of integral flux at energies  $\geq 1$  TeV vs. orbital phase ( $\phi$ ) shows an almost sinusoidal behaviour, with the bulk of the emission largely confined in a phase interval  $\phi \sim 0.45$  to  $0.9$ , covering about half of the orbital period. The emission maximum ( $\phi \sim 0.7$ ) appears to lag behind the apastron epoch and to align better with the *inferior conjunction* ( $\phi = 0.716$ ), when the compact object lies in front of the massive star (see Fig. 1). The VHE flux minimum occurs at phase ( $\phi \sim 0.2$ ), slightly further along the orbit

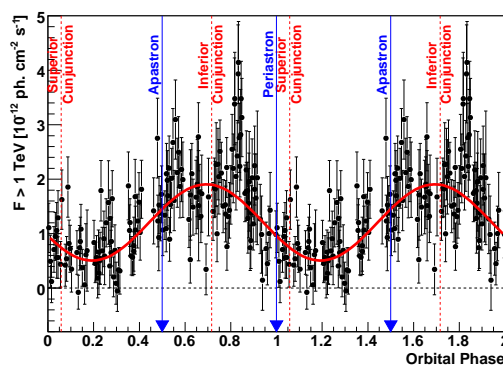


Figure 3: Phasogram (Integral run-by-run  $\gamma$ -ray flux above 1 TeV as function of orbital phase) of LS 5039 from H.E.S.S. data from 2004 to 2005. Each run is  $\sim 28$  minutes. Two full phase periods are shown for clarity. The vertical blue arrows depict the respective phases of minimum (*periastron*) and maximum (*apastron*) binary separation. The vertical dashed red lines show the respective phases of inferior and superior conjunction, when the star and the compact object are aligned along the observer's line of sight. From [9].

than *superior conjunction* ( $\phi = 0.058$ ). Neither evidence for long-term secular variations nor any other modulation period are found in the presented H.E.S.S. data.

## Spectral Modulation

Due to the changing environment with orbital phase (magnetic field strength, stellar photon field, relative position of compact object and star with respect to observer, ...), the VHE  $\gamma$ -ray emission spectrum is expected to vary along the orbit.

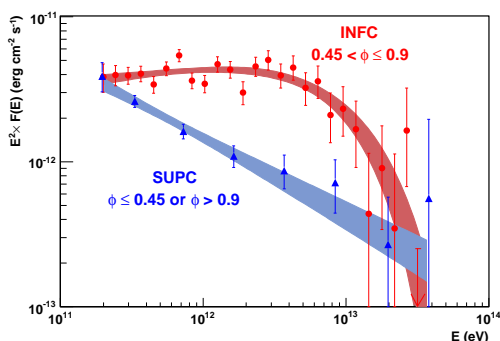


Figure 4: Very high energy spectral energy distribution of LS 5039 for the two broad orbital phase intervals defined in the text, **INFC** (red circles) and **SUPC** (blue triangles). The shaded regions represent the  $1\sigma$  confidence bands on the fitted functions. A clear spectral hardening is occurring in the 200 GeV to a few TeV range during the **INFC** phase interval. From [9].

We first define two broad phase intervals: **INFC** centered on the inferior conjunction ( $0.45 < \phi \leq 0.9$ ) and its complementary **SUPC** centered on the superior conjunction, corresponding respectively to high and low flux states. The high state VHE spectral energy distribution (Fig 4) is consistent with a hard power law with index  $\Gamma = 1.85 \pm 0.06_{\text{stat}} \pm 0.1_{\text{syst}}$  and exponential cutoff at  $E_0 = 8.7 \pm 2.0$  TeV. In contrast, the spectrum for low state is compatible with a relatively steep ( $\Gamma = 2.53 \pm 0.06_{\text{stat}} \pm 0.1_{\text{syst}}$ ) pure power law extending from 200 GeV to  $\sim 20$  TeV. Interestingly, the flux appears to be almost unmodulated at 200 GeV as well as around 20 TeV, whereas the modulation is maximum around a few ( $\sim 5$ ) TeV.

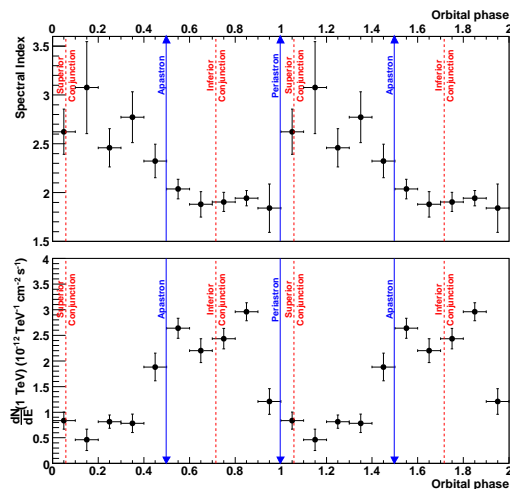


Figure 5: Top: Fitted pure power-law photon index vs. phase interval of width  $\Delta\phi = 0.1$ . Bottom: Differential flux at 1 TeV for the same phase interval. From [9].

Looking at smaller phase intervals, Fig 5 shows the results of a pure power-law fit of the high energy spectra in 0.1 orbital phase bins (restricted to energies below 5 TeV to avoid systematic effect introduced by the high state cutoff). The flux normalisation at 1 TeV (bottom) and photon index (top) are strongly correlated, the flux being higher when the spectrum is harder and vice-versa.

## Interpretation and Conclusion

The basic paradigm of VHE  $\gamma$ -ray production requires the presence of particles accelerated to multi-TeV energies and a target comprising photons (for  $\gamma$ -ray production through the Inverse Compton effect) and/or matter of sufficient density (for  $\gamma$ -ray production through pion decay in hadronic processes). Several model classes are available to explain VHE emission from gamma-ray binaries, differentiating one from the other by the nature of accelerated particles and/or the location of the acceleration region. In jet-based models, particle acceleration could take place directly inside and along the jet, e.g. [11, and references therein], and also in the jet termination shock regions [12]. Non-jet scenarios are also available, e.g. [13, 14], where the emission arises from the

interaction of a pulsar wind with the stellar companion equatorial wind.

New observations by HESS have established orbital modulation of the VHE  $\gamma$ -ray flux and energy spectrum from the XRB LS 5039. The observed VHE modulation indicates that the emission most probably takes place close (within  $\sim 1$  AU) to the massive stellar companion, where modulated  $\gamma$ -ray absorption via pair production ( $e^+e^-$ ) on the intense stellar photon field is unavoidable (e.g. [14]). The observed spectral modulation is however incompatible with a pure absorption scenario, which in particular predicts a maximum variability around 300 GeV and a VHE spectral hardening in the low flux state, inconsistent with observations.

Modulation could also arise from a modulation of the acceleration and cooling timescales along the orbit due to varying magnetic field and photon field densities (e.g. [9, and references therein]) which could modify the maximum electron energy and therefore induce a phase-dependent energy break in the  $\gamma$ -ray spectrum. Modulation of the accretion rate due to interaction of the stellar wind with the compact object in the microquasar scenario (e.g. [15]) could be another ingredient of the observed modulation. A detailed study is now required to fully explain these new observations and understand the complex relationship between  $\gamma$ -ray absorption and production processes within these binary systems.

## Acknowledgements

The support of the Namibian authorities and of the University of Namibia in facilitating the construction and operation of H.E.S.S. is gratefully acknowledged, as is the support by the German Ministry for Education and Research (BMBF), the Max Planck Society, the French Ministry for Research, the CNRS-IN2P3 and the Astroparticle Interdisciplinary Programme of the CNRS, the U.K. Particle Physics and Astronomy Research Council (PPARC), the IPNP of the Charles University, the South African Department of Science and Technology and National Research Foundation, and by the University of Namibia. We appreciate the excellent work of the technical support staff in Berlin, Durham, Hamburg, Heidelberg, Palaiseau, Paris,

Saclay, and in Namibia in the construction and operation of the equipment.

## References

- [1] I. Mirabel, L. Rodriguez, *Nature* 371 (1994) 46.
- [2] C. Motch, F. Haberl, K. Dennerl, et al., *A&A* 323 (1997) 853–875.
- [3] J. Marti, J. M. Paredes, M. Ribó, *A&A* 338 (1998) L71–L74.
- [4] J. M. Paredes, J. Martí, M. Ribó, et al., *Science* 288 (2000) 2340–2342.
- [5] F. Bosch-Ramon, J. Paredes, M. Ribó, *ApJ* 628 (2005) 388.
- [6] J. Casares, M. Ribó, I. Ribas, J. others Paredes, et al., *MNRAS* 364 (2005) 899.
- [7] F. Aharonian (HESS Collaboration), *A&A* 457 (2006) 899–915.
- [8] F. Aharonian (HESS Collaboration), *Science* 309 (2005) 746.
- [9] F. Aharonian (HESS Collaboration), *A&A* 460 (2006) 743–749.
- [10] J. D. Scargle, *ApJ* 263 (1982) 835–853.
- [11] F. Bosch-Ramon, J. Paredes, *A&A* 417 (2004) 1075.
- [12] S. Heinz, R. Sunyaev, *A&A* 390 (2002) 751–766.
- [13] L. Maraschi, A. Treves, *MNRAS* 194 (1981) 1.
- [14] G. Dubus, *A&A* 456 (2006) 801.
- [15] J. M. Paredes, V. Bosch-Ramon, G. E. Romero, *A&A* 451 (2006) 259–266.